



OPEN **Bioinformatics Identification of angiogenesis-related biomarkers and therapeutic targets in cerebral ischemia-reperfusion**

Yong-Hong Wu^{1,2}, Jing Sun², Jun-Hua Huang² & Xiao-Yun Lu¹✉

Promoting vascular endothelial cell regeneration can enhance recovery from cerebral ischemia reperfusion injury (CIRI), but there is a lack of bioinformatic studies on angiogenesis-related biomarkers in CIRI. In this study, we utilized the GSE97537 and GSE61616 datasets from GEO to identify 181 angiogenesis-related genes (ARGs) and analyzed differentially expressed genes (DEGs) between CIRI and control groups. We converted ARGs to 169 rat homologues and intersected them with DEGs to find DE-ARGs. RF and XGBoost models were employed to identify five biomarkers (Stat3, Hmox1, Egfr, Col18a1, Ptgs2) and conducted GSEA on these biomarkers, revealing their enrichment in pathways such as ECM-receptor interaction and hematopoietic cell lineage. We also analyzed the immune microenvironment, finding significant differences in 21 immune cells between CIRI and control groups. Furthermore, we constructed lncRNA-miRNA-mRNA networks and drug-gene networks. Finally, biomarker expression was compared between the CIRI and control groups by qRT-PCR in tissue and blood samples. Overall, our bioinformatic exploration of angiogenesis-related biomarkers in CIRI provides new insights for the diagnosis and treatment of CIRI.

Keywords Cerebral ischemia reperfusion injury, Angiogenesis, Gene expression omnibus, Bioinformatic

When the blood supply is restored after a certain period of cerebral ischemia, the degree of brain injury is often further aggravated than that of ischemia, and more serious brain dysfunction often appear¹. In the ischemic cerebral region, Reperfusion and restoration of the blood supply often result in a series of cellular and biochemical consequences, including generation of reactive oxygen species (ROS), inflammatory cytokines, further cause inflammation, and cerebral cell damage, which is known as cerebral ischemia-reperfusion injury (CIRI)². CIRI is an important factor leading to poor prognosis in patients with Cerebral ischemic stroke (CIS)³.

So far, diagnosis and severity assessment of CIRI almost exclusively relies on a patient's neurologic presentation, CT, MRI and other imaging examinations, which has limitations and deficiencies due to time consuming, differences in experience of examining doctor and the backward equipment of Grass-roots hospital⁴. In addition, some patients could not perform dynamic imaging observation because of their critical condition. Biomarkers play an important role in the diagnosis, progression and prognosis of many diseases due to their convenient fast measurement, reliability, and low cost. Regrettably, biomarkers are rarely used in CIRI and there are no ideal biomarkers for detecting CIRI at present. To date, mRNAs have been studied as potential diagnostic biomarkers for stroke⁴. many mRNAs are differentially expressed in the various conditions of the same disease or different diseases but an accurate distinction of each specific condition from the others could not be done using a single mRNA⁴. Furthermore, also because the pathogenesis of CIRI is complex and there are many influencing factors, the study of screening out a group of genes rather than only a gene and obtaining their gene expression profile is indispensable to fully characterize CIRI in order to screen effective biomarkers. At present, only a few studies have shown that some RNA biomarkers have certain diagnostic values for stroke and transient ischemic stroke. In a human study, mRNA expression profile of a panel containing 18 genes detected in whole blood was used to discriminate acute strokes from controls with a specificity of 89.5% and a sensitivity of 93.5%⁵. Further human studies demonstrated that differential expression genes (DEGs) had a sensitivity and a specificity of 100%

¹Key Laboratory of Biomedical Information Engineering of Ministry of Education, School of Life Science and Technology, Xi'an Jiaotong University, Xi'an 710049, Shanxi Province, China. ²School of Medical Technology & Institute of Basic Translational Medicine, Xi'an Medical University, Xi'an 710021, Shanxi Province, China. ✉email: ywhguilai11@163.com

for diagnosis of the transient ischemic stroke^{6,7}. However, there are relatively few studies on the application of RNA biomarkers in CIRI, so it is essential to find new RNA biomarkers to diagnose and treat CIRI.

Angiogenesis is a process in which endothelial cells are directly or indirectly activated by angiogenesis factors to form new blood vessels on the basis of original vessels. Angiogenesis is affected cooperatively by pro-angiogenesis factors and anti-angiogenesis factors, and internal and external factors such as ischemia and hypoxia can influence angiogenesis. Angiogenesis is closely related to the occurrence and development of CIRI. Angiogenesis is one of the mechanisms that promote cell survival for neurorestoration and cell survival⁸. As a crucial process and a natural defense mechanism, Angiogenesis contributes to restoring oxygen and nutrient supply to the ischemic brain tissue^{9,10}. They are favourable to save endangered brain tissue and enhance brain tissue function. Angiogenesis can promote the formation of collateral circulation and guarantee the structural and functional integrity of cerebral arteries^{11,12}. Moreover, it provides a key neurovascular substrate for neuronal remodeling, and can restore local cerebral blood supply in time, which is crucial for functional recovery after CIRI¹³. In recent years, a large number of studies have found that increased vascular density in brain tissue is associated with improved prognosis of CIRI¹⁴. Angiogenesis is a key factor affecting good recovery after CIRI¹⁵. Those CIS patients with greater cerebral blood vessel density in the ischemic border show better survival⁹. Studies have indicated that promoting the regeneration of vascular endothelial cells (ECs) is key to accelerating angiogenic response, restoring blood supply to ischemic lesions, rescuing dead neurons and glial cells, and improving the recovery of CIRI¹⁶. As the major effector cells of the neovascularization, ECs around the infarcted brain region start to proliferate 12 to 24 h after cerebral ischemia¹⁷. Most of the well-known angiogenic factors increased as early as 1 h. The evidence strongly suggests that angiogenesis occurs immediately after CIRI¹⁰.

In the field of modern medical therapies, especially for anti-angiogenic therapies, biomarker studies are of irreplaceable importance in the development of personalized treatment plans¹⁸. With the development of medicine, we gradually realize that there are significant differences in the response of different patients to the same treatment, and this difference is not only related to the physiological characteristics of the individual, but also closely related to the specific biomarkers and drug resistance mechanisms in the patient. By delving into the biomarkers as well as the mechanisms of resistance, we are able to tailor treatment to a patient's unique circumstances. If these biomarkers can be accurately identified, doctors can select the most effective drugs for sensitive patients and improve treatment outcomes; At the same time, for patients who may develop drug resistance, treatment strategies can be adjusted in advance to avoid ineffective treatment and reduce the generation of drug resistance. This not only helps to improve the survival rate and quality of life of patients, but also makes more rational use of medical resources to avoid unnecessary side effects of drugs and waste of medical expenses^{18,19}.

To sum up, angiogenesis biomarkers may have great potential and value for early diagnosis of CIRI, assessment of severity, progression, therapeutic effect and prognosis of CIRI. However, the expression level of genes associated with angiogenesis as biomarkers of CIRI and their potential molecular mechanisms have not been reported.

Here, based on the GEO database, our study aimed to explore potential angiogenesis-related biomarkers of CIRI, provide important biological information for the early diagnosis and new targets for therapeutic drug screening and developing. The study provided a new idea for future clinical research and contributed to revealing the possible pathogenesis.

Results

A total of 38 DE-CPRGs were identified

There were 914 DEGs between CIRI and control samples (Fig. 1a, Table S2). Figure 1b illustrated the top10 up- and down-regulated DEGs. 38 DE-ARGs were yielded after taking intersection of DEGs with rat homologous genes ($n = 169$) (Fig. 1c). The GO entries involved in DE-ARGs containing regulation of vasculature development, epithelial cell migration, regulation of endothelial cell migration, cellular response to transforming growth factor beta stimulus, regulation of blood coagulation et al. (Fig. 1d, Table S3). The KEGG pathways enriched by DE-ARGs covered ECM-receptor interaction, HIF-1 signaling pathway, signaling pathways regulating pluripotency of stem cells, lipid and atherosclerosis, etc. (Fig. 1e, Table S4).

Stat3, Hmox1, Egfr, Col18a1 and Ptgs2 were identified as biomarkers

A total of 18 and 6 genes were gained by RF and XGBoost, respectively (Fig. 2a-b). Five biomarkers namely Stat3, Hmox1, Egfr, Col18a1 and Ptgs2 were derived after taking the intersection of genes obtained by RF and XGBoost (Fig. 2c), and they were all differentially expressed between CIRI and control samples in the two datasets, in which Ptgs2 expressed an opposite trend in the two datasets (Fig. 2d and e). The area under the curve (AUC) of Stat3, Hmox1, Egfr, Col18a1 and Ptgs2, were all greater than 0.7 both the training and validation sets, indicating their high diagnostic value for CIRI (Fig. 2f, Figure S2).

Pancreatic adenocarcinoma was the most significantly activated pathway by IPA

Pancreatic adenocarcinoma signaling was found to be the most significantly activated pathway by IPA (Fig. 3a-b). Stat3 was enriched to functional pathways such as ECM-receptor interaction, P53 signaling pathway, NOD like receptor signaling pathway (Fig. 3c, Table S5). Protein interaction results showed that Stat3 had strong interaction with three other biomarker genes (Egfr, Hmox1 and Ptgs2), but Col18a1 was a free point, no interaction was observed (Figure S1a). Changes in upstream and downstream molecule expression associated with the STAT3 signaling pathway are showed in Figure S1b. As shown in it, the STAT3 signaling pathway is activated as a whole. Cell growth factor - cell growth factor receptor, which in turn activates JAK2 SRC, which in turn activates STAT3 (phosphorylation). In addition, cytokines and cytokine receptors activate JAK2, which in turn activates STAT3. After that, STAT3 activates PIM1-BCL2 to induce anti-apoptosis and affect cell growth, survival and

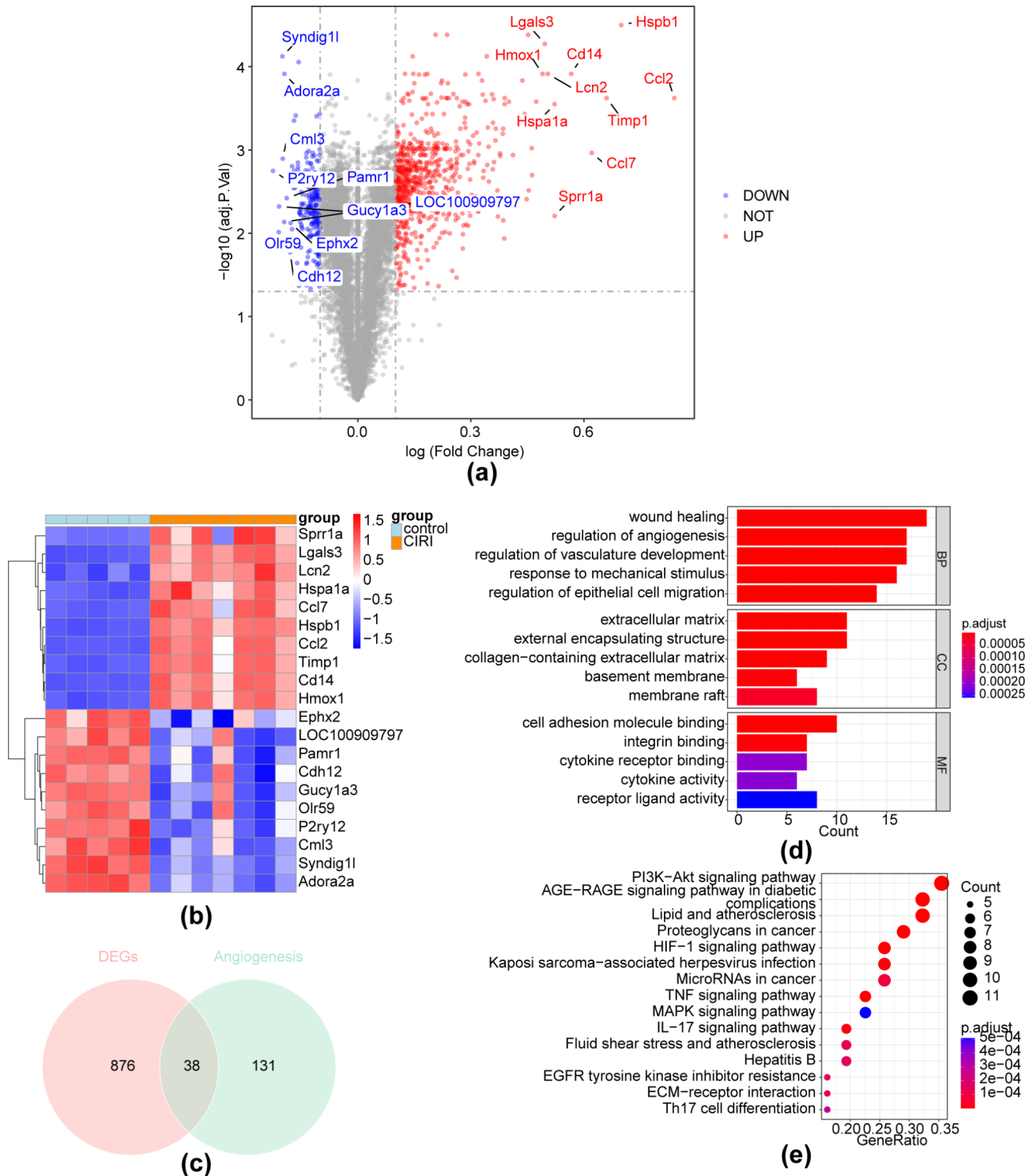


Fig. 1. Identification of differentially expressed angiogenesis-related genes (DE-ARGs). **(a)** Volcano plot showing DEGs between CIRI and control samples; **(b)** Heatmap of the expression levels of up-regulated and down-regulated genes in the CIRI and control groups. Red and blue squares indicate activation and suppression, respectively; **(c)** Venn diagram showing the intersection of DEGs and ARGs in the dataset; **(d)** GO enrichment analysis for DE-ARGs; **(e)** KEGG enrichment analysis for DE-ARGs.

differentiation. In addition, the activation of STAT3 caused MYC activation and thus activated CDC25A, which further caused the transformation of G1 into S phase. In addition, STAT3 can also activate transcription, which causes a series of downstream changes. The 6 genes Cdkn1a, Jak2, Myc, Ptpn2, Ptpn6 and Stat3 were yielded after taking intersection of DEGs with the genes associated with STAT3 signaling pathway (Figure S1c). Hmx1

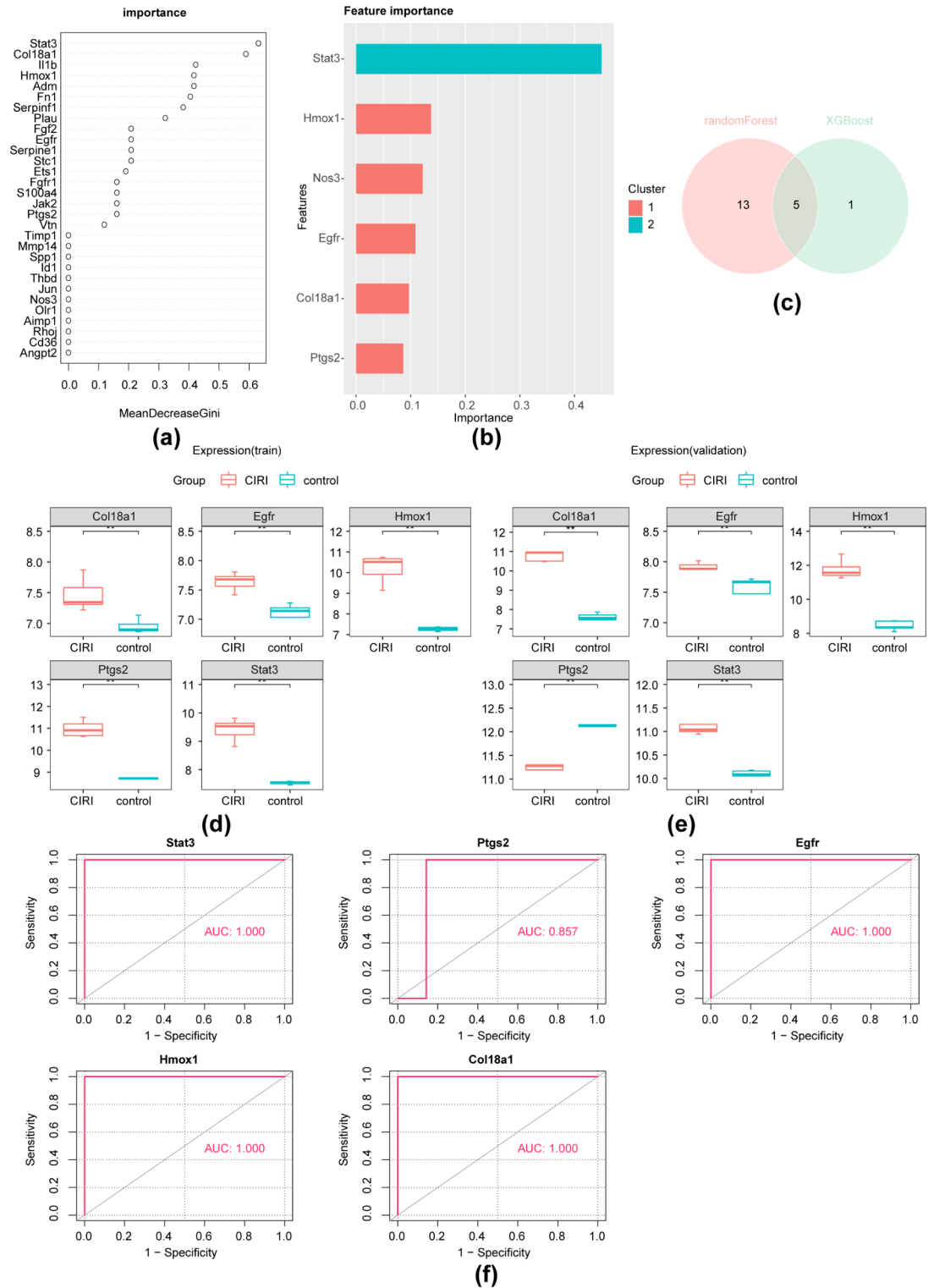


Fig. 2. Identification of biomarkers from DE-ARGs. **(a)** Importance plot of candidate biomarker genes in the random forest model (RF); **(b)** Importance of the matrix plot of candidate biomarker genes in the XGBoost model; **(c)** Venn diagram showing the intersection of genes obtained by RF and XGBoost; **(d)** Boxplot showing differences in expression of five candidate biomarkers between CIRI and control samples in GSE97537; **(e)** Boxplot showing differences in expression of five biomarker genes between CIRI and control samples in GSE134347 (** $p < 0.01$); **(f)** ROC curve of candidate biomarker genes for diagnosis (AUC > 0.8).

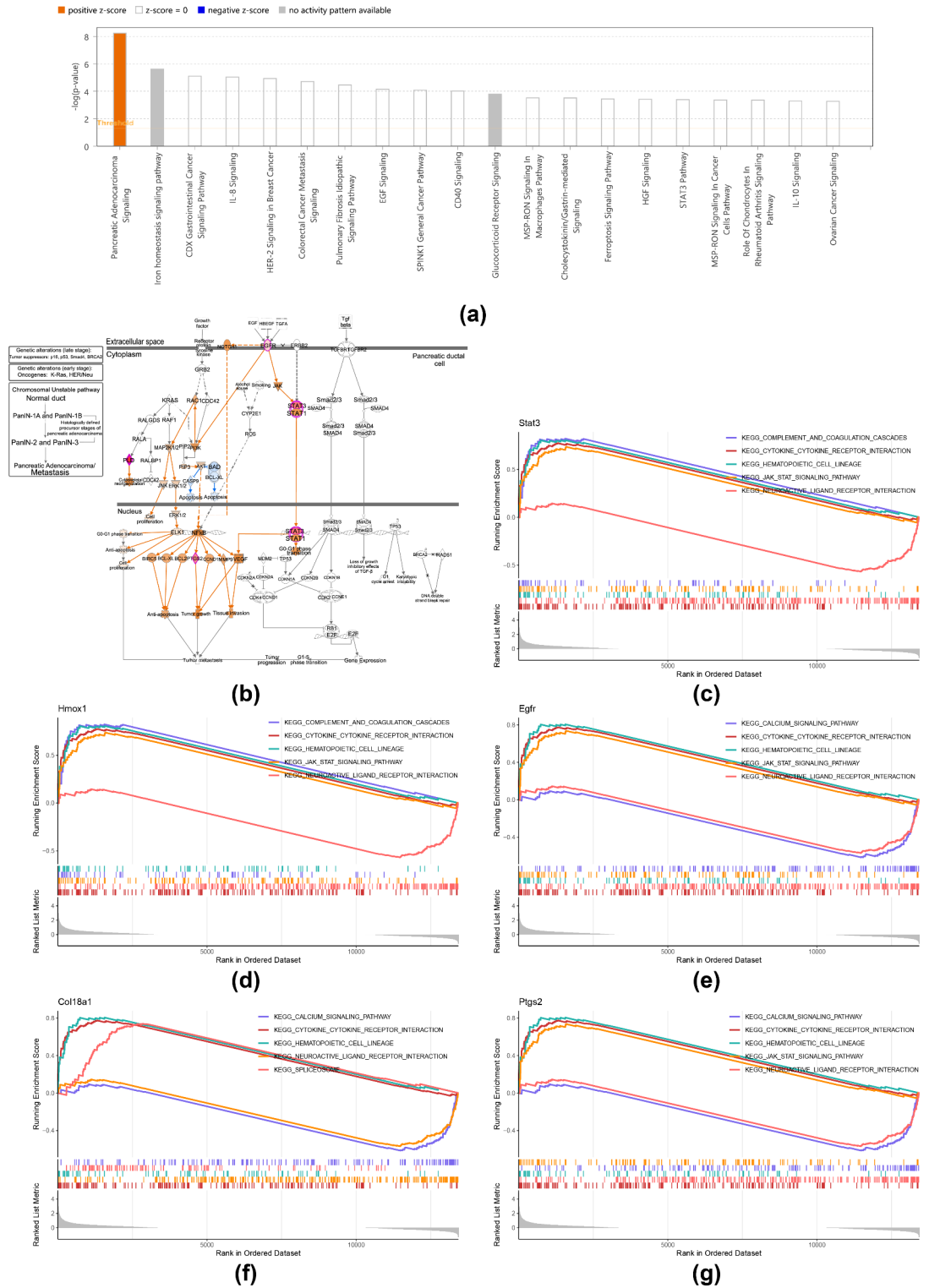


Fig. 3. The results of IPA and GSEA based on biomarkers. **(a)** Significant classical pathway enrichment results ($p < 0.05$); **(b)** Pancreatic adenocarcinoma signaling transduction pathway. Molecules that are relevant to the experimental dataset are highlighted in pink. The up and down-regulation of these molecules in the experiment is shown in red and green, respectively. Some molecules have a double border. Such icons refer to protein complexes or protein families, members of which are molecules in the data set. The orange arrow represents the activated process, the blue represents the inhibited process, and the yellow represents the inconsistency with state of downstream molecule; **(c-g)** GSEA results showing five pathways change associated with changes in *stat3*, *Hmox1*, *Egfr*, *Col18a1*, and *Ptg22* expression levels. The five pathways that each biomarkers is involved in are the smallest in order of p_{adjust} .

was involved in complement and coagulation cascades, calcium signaling pathway, neuroactive ligand receptor interaction, etc. (Fig. 3d, Table S5). Egfr was associated with apoptosis, hematopoietic cell lineage, JAK stat signaling pathway, etc. (Fig. 3e, Table S5). Col18a1 was participated in cytokine cytokine receptor interaction, spliceosome, calcium signaling pathway, etc. (Fig. 3f, Table S5). Ptgs2 was enriched to the functional pathways including cell cycle, focal adhesion, chemokine signaling pathway, etc. (Fig. 3g, Table S5).

Biomarkers are highly expressed in different tissues

Egfr and Stat3 had the highest expression levels in amygdala tissues, the expression level of Hmox1 was highest in spleen, while Ptgs2 expression level was highest in hippocampus (Fig. 4a). The expression levels of Egfr, Stat3, Hmox1 and Ptgs2 were all very high in endothelial cell (Fig. 4a). The PPI network contained Col18a1-BLVRB, Egfr-EPS8, Stat3-ABL1 and other reciprocal relationship pairs (Fig. 4b).

Significant differences in immune cells

To understand immune cell infiltration between CIRI and control samples, ssGSEA analyses were performed. The heat map results show that demonstrated the abundance of immune cells in the training set (Fig. 5a). There were 21 immune cells with remarkably different expression between CIRI and control samples, such as activated CD4 T cell, activated dendritic cell and central memory CD4 T cell (Fig. 5b). Five biomarkers showed a strong positive correlation with most of the remarkably differentially expressed immune cells, only monocyte and neutrophil had a strong negative correlation with the biomarkers (Fig. 5c).

Stat3, Homx1, Egfr and Ptgs2 predicted 2, 13, 34 and 106 drugs respectively

We finally predicted 662 miRNAs and 1 lncRNA targeting AABR07021544.1. Hence, 4 mRNAs, 1 miRNA and 1 lncRNA constituted the lncRNA-miRNA-mRNA network, which included AABR07021544.1-rno-miR-125b-5p-Hmox1, AABR07021544.1-rno-miR-125b-5p-Ptgs2, AABR07021544.1-rno-miR-125b-5p-Egfr and other relationship pairs (Fig. 6a). Through drug prediction, Stat3, Homx1, Egfr and Ptgs2 respectively correspond to 2, 13, 34 and 106 drugs. The drug-target network contained Formic acid-Homx1, Cetuximab-Egfr, Icosapent-Ptgs2, etc. (Fig. 6b).

Hmox1, Egfr, Col18a1 and Ptgs2 were significantly upregulated in blood and tissue

Compared to the Control group in blood and tissue samples, Hmox1, Egfr, Col18a1 and Ptgs2 were all significantly up-regulated in the CIRI group (Fig. 7a-b). The expression trends of these 4 biomarkers were consistent with the results in training set.

Discussion

CIS has a high probability of death, disability and recurrence, a long course of disease, a huge cost of medical resources, and a serious burden on families and society. After CIS, long-term CIRI can cause a series of pathological injuries such as apoptosis, autophagy, necrosis and necrotic apoptosis²⁰, which lead to brain dysfunction, systemic inflammatory response syndrome and other serious clinical manifestations. CIRI plays an important role in the course of CIS, but the specific mechanism leading to CIRI is still unclear. Currently, there is still a lack of effective drugs for the treatment of CIRI due to the lack of effective targets for drug screening. Therefore, screening effective drug targets has become an urgent problem to be solved. Almost every neuron has its own independent supply of blood vessels²¹. Blood vessels carry oxygen, energy, and nutrients to nourish neurons, and carry away the waste neurons release. After the development of CIR, in the ischemic penumbra tissue, a variety of angiogenic factors are released to initiate and regulate angiogenesis, this contributes extremely to anti-injury and post-injury repair after CIR. Because angiogenesis can play a positive therapeutic role by promoting neurogenesis, improving nerve function and other mechanisms, its treatment of cerebral ischemia has been considered and recognized²². The study of ARGs as biomarkers can not only provide ideas for further exploring the mechanism of CIRI, but also provide potential candidate drug targets for its treatment. We identified five angiogenesis related biomarkers, namely Stat3, Hmox1, Egfr, Col18a1 and Ptgs2, for CIRI. Numerous reports in the literature suggest the functions of these five genes were associated with the response to CIRI.

EGFR with intrinsic tyrosine kinase activity is one of the main members of the tyrosine kinase receptor family²³. Activating EGFR can result in various effects including migration, proliferation, differentiation, antiapoptosis, and angiogenesis through activating its downstream signal pathway²⁴. Recent studies showed that activating EGFR ameliorates CIRI²⁵. A study demonstrated that EGFR was phosphorylated and transactivated during both ischemia and reperfusion periods²⁶. Our results also indicated that the expression level of Egfr increased after CIRI. We speculated that EGFR was activated, thereby stimulating intracellular signaling cascades to exert neuroprotective effects in CIRI patients. Neuroactive ligand-receptor interaction, ECM-receptor interaction and endocytosis were identified as the top three biological processes related to Danhong injection treatment caused by CIRI, and the activities of these three pathways are closely related to CIRI²⁷. Our results also indicated that Egfr is related to neuroactive ligand receptor interaction, hematopoietic cell lineage, JAK-STAT signaling pathway and so on. Hematopoietic stem cells transplantations at 2 h and 24 h after the reperfusion in MCAO mice has been shown to have neuroprotective effects that is likely dependent on the secretion of growth factors²⁸, accompanied by activation of the hematopoietic stem cell lineage signaling pathway. In addition, vascular endothelial growth factor (VEGF) has been identified as a key mediator of angiogenesis that supports tumorigenesis. Egfr enrichment results suggest that the activity of VEGF receptor on vascular endothelial cells may be altered due to Egfr's regulation of neuroactive ligand-receptor interactions, thereby affecting VEGF-induced proliferation, migration and other key steps in angiogenesis²⁹. The effects of JAK2/STAT3 signaling pathway in CIRI are described below for STAT3.

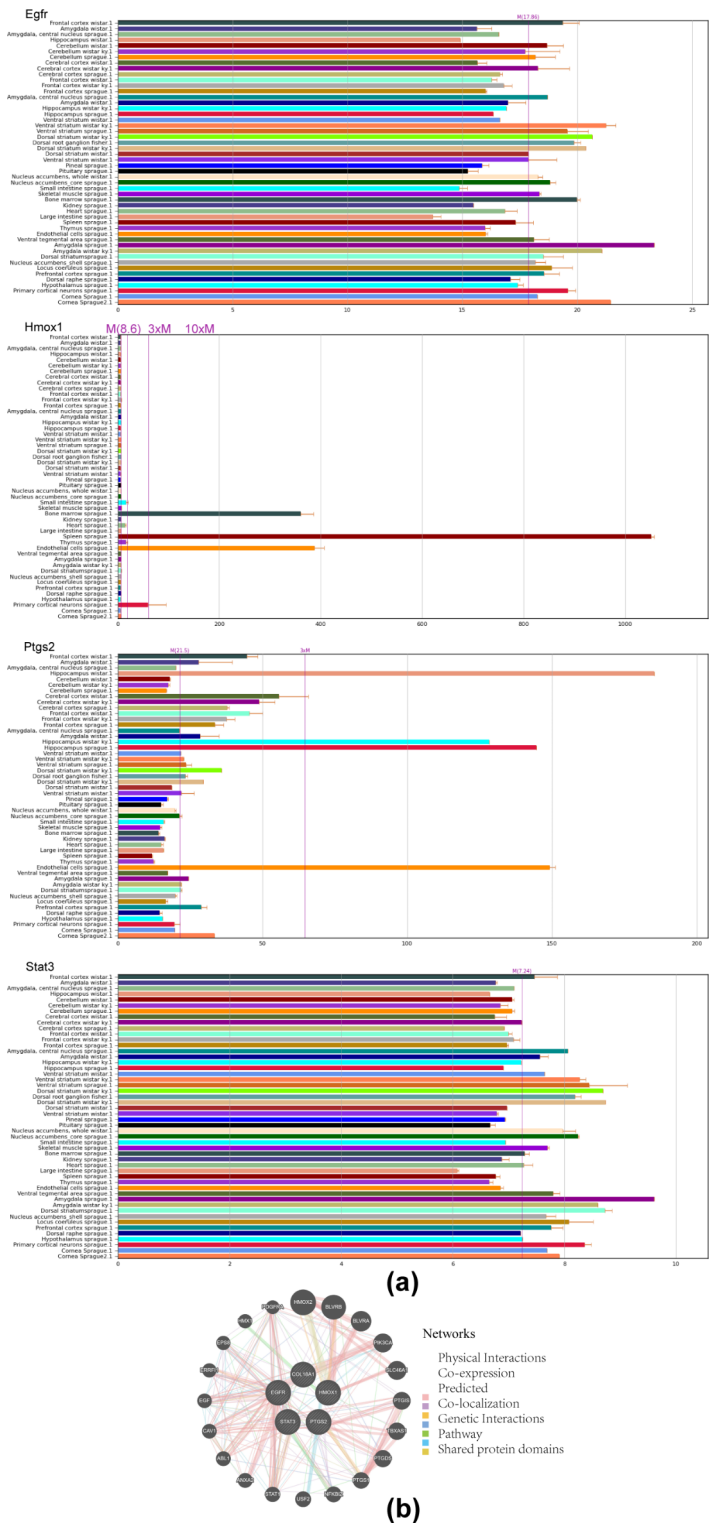


Fig. 4. Tissue specific expression and PPI network of biomarkers. **(a)** Specific expression levels of Egrf, Hmx1, Ptg2 and Stat3 in different tissues. No tissue-specific expression information was found for Col18a1; **(b)** The relationship network between biomarkers (Egfr, Hmx1, Ptg2, Col18a1 and Stat3) and other related genes.

The Hmx1 is rapidly induced and activated by a wide range of pro-oxidant and inflammatory stimuli. Hmx1 encodes heme oxygenase 1 (HO-1) which is essential in heme catabolism. studies demonstrated that, in the brain, HO-1 induced by stroke activates Nrf2 to play a variety of protective roles including antiapoptosis, antiinflammatory, antioxidation and vasodilation²⁸. A recent study indicated that expression levels of the HO-1

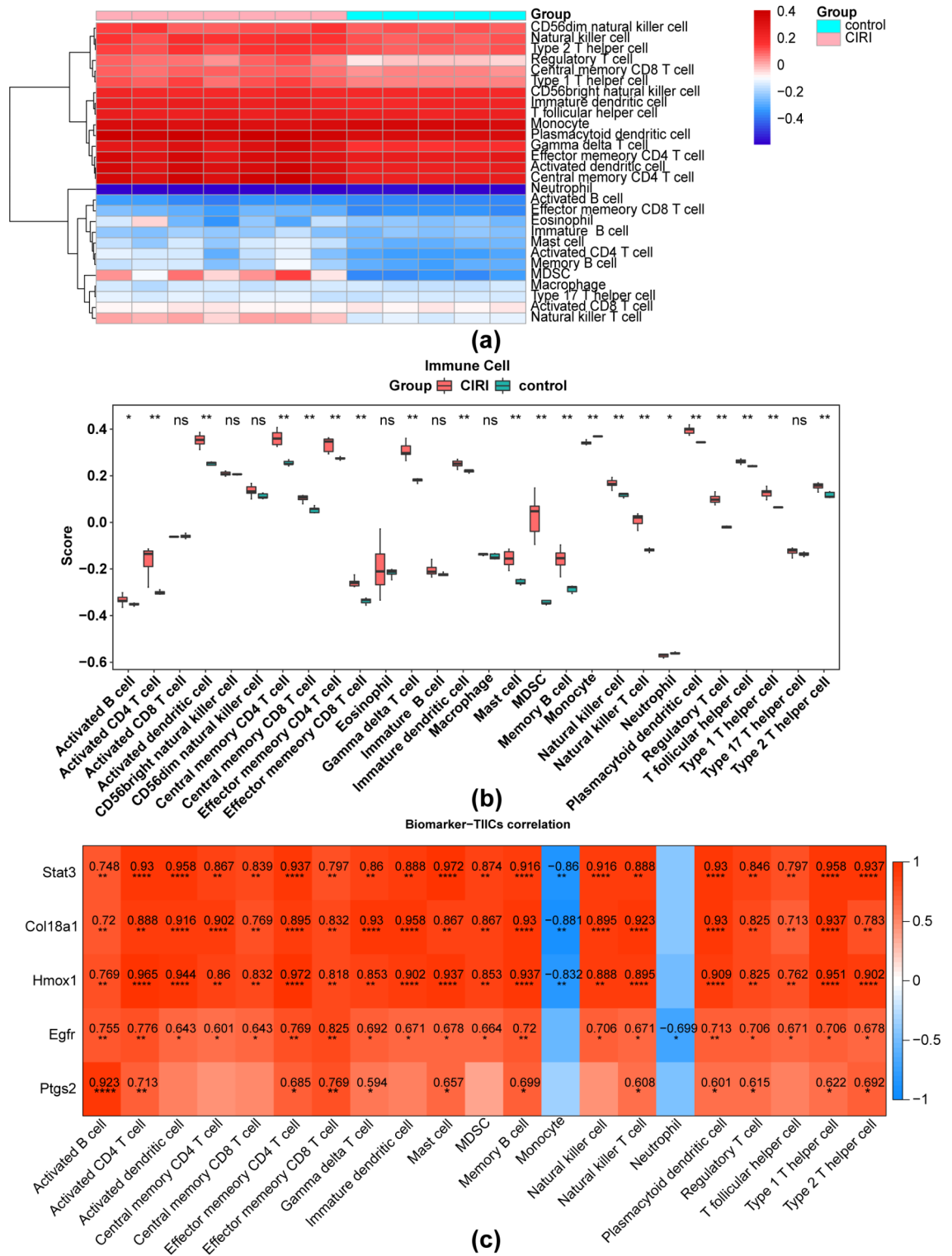


Fig. 5. The expression of biomarkers in immune cells and its correlation with the remarkably differentially expressed immune cells between CIRI and control samples. **(a)** Heat map of biomarker expression levels in immune cells; **(b)** Boxplot showing differences in expression of the 5 biomarkers in 28 immune cells between CIRI and control samples (* $p < 0.05$, ** $p < 0.01$, ns: no significant difference); **(c)** Correlation of biomarkers and immune cells with remarkably different expression between the two samples. Blue squares represent the negative correlation; red squares represent the positive correlation.

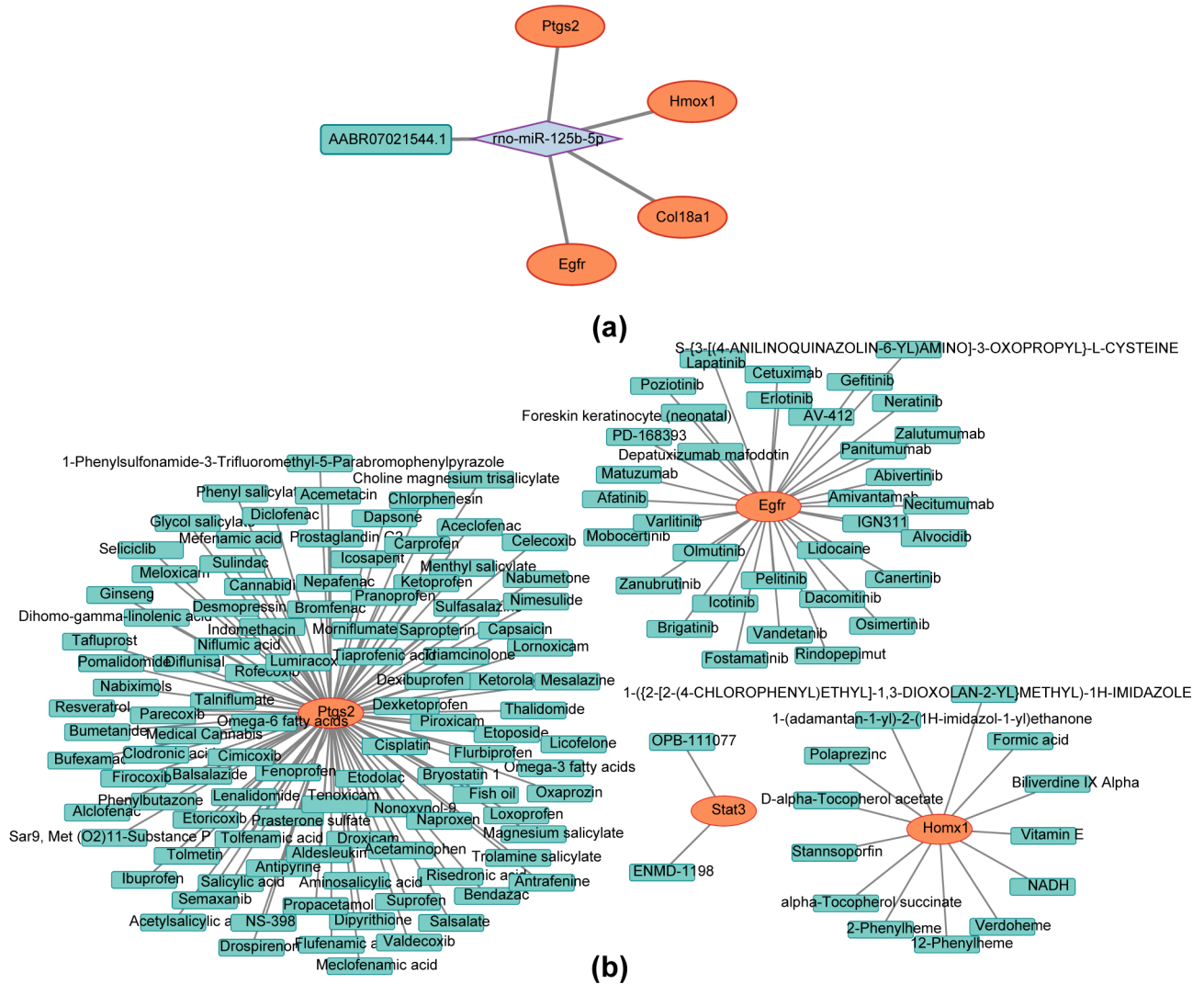


Fig. 6. CeRNA network and drug prediction analysis based on biomarkers. **(a)** LncRNA-miRNA-mRNA network. The cyan rectangles represent lncRNA, the gray diamonds represent miRNA, and the orange ovals represent biomarkers, **(b)** Network based on drug-target prediction. The cyan rectangles represent potential drugs of targeting biomarkers.

after CIRI were negatively correlated with the extent of ferroptosis, and HO-1 improved cognitive impairment³⁰. In a study, ROC monofactor analysis demonstrated a good performance of Hmox1, Stat3 as ferroptosis-related genes in the diagnosis of CIR³¹. Interestingly, our results of the ROC analysis also show a good performance of Hmox1, Stat3 as angiogenesis-related genes in the diagnosis of CIR. The complement and coagulation cascade signaling pathways mediate inflammatory responses in CIR³². In addition, although the relationship between Leishmania infection and CIR has not been reported in literature, Leishmania infection can result in NLRP3 inflammasome activation in macrophages³³. Interestingly, NLRP3 inflammasome also is activated in CIR. Our results also suggested that Hmox1 was involved in complement and coagulation cascade, calcium signaling pathway, Leishmania infection and other KEGG pathways. The activation of HMOX1 facilitates VEGF- and stromal-derived growth factor-1(SDF-1)-driven angiogenesis and wound healing, while protecting against inflammatory angiogenesis, however, the HMOX1 activity favors tumor angiogenesis and metastasis that is suggested by increasing findings³⁴. At the same time, regulating the activity of calcium channel protein or calcium-binding protein in calcium signaling pathway can affect calcium homeostasis in endothelial cells, which has also been confirmed by Lin et al.³⁵.

Col18a1 encodes the collagen type XVIII $\alpha 1$ chain that is a widely expressed, non-fibrillar collagen associated with vascular and epithelial basement membranes³⁶. Collagen XVIII is needed for normal brain development³⁶. The angiogenesis inhibitor endostatin is a 20 kDa C-terminal fragment of collagen XVIII. Plasma endostatin and VEGF levels were elevated in stroke patients compared to healthy volunteers³⁷. A study indicated that an increase in levels of plasma endostatin was associated with cognitive deficit at 3 months after CIS, prompting that endostatin may be a meaningful biomarker for cognitive deficit after CIS³⁸. Another study showed that elevation in levels of plasma endostatin in acute IS was associated with an increase in risk of severe disability and mortality

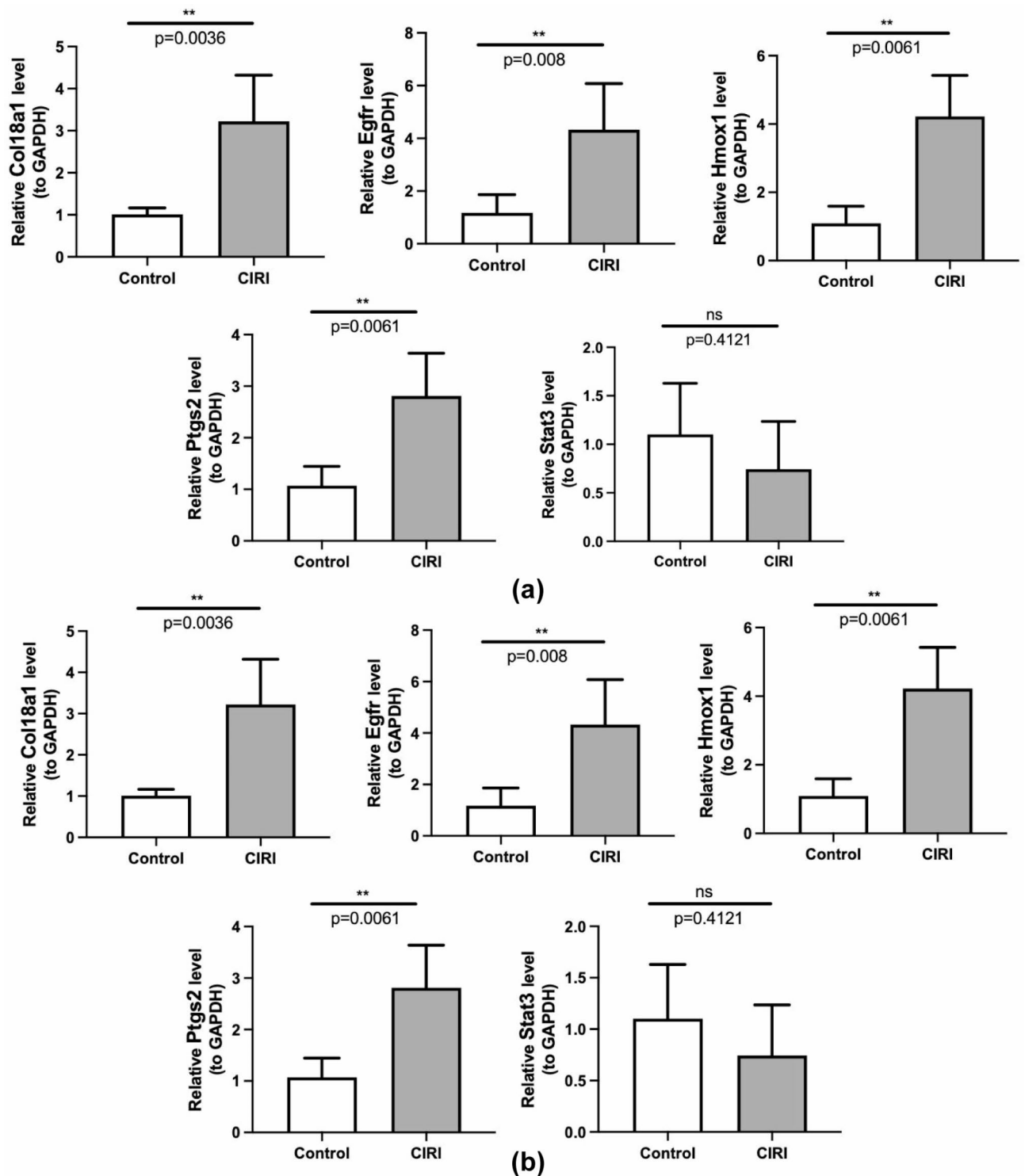


Fig. 7. Results of RT-qPCR for the five biomarkers ($*p < 0.05$, $**p < 0.01$, $***p < 0.001$, ns: no significant difference). **(a)** The results between CIRI and control sample of the whole blood; **(b)** The results between CIRI and control sample of the brain tissue.

at 3 months, so plasma endostatin was regarded as a potentially important prognostic marker for risk stratification in patients suffering from IS³⁹. Numerous genes involved in the KEGG pathway of neuroactive ligand-receptor interaction were differentially expressed in CIRI²⁷. Interestingly, the results in our study indicated that Col18a1 was involved in neuroactive ligand receptor interaction, cytokine-cytokine receptor interaction, hematopoietic cell lineage and so on. This suggests that Col18a1 may indirectly affect the expression of key angiogenic factors

such as VEGF by regulating the release of neuroactive ligands or the sensitivity of receptors, thereby changing the rate and quality of angiogenesis and thus affecting the formation of blood vessels in the brain⁴⁰.

In the study, these biomarkers predicted different amounts of the drug. Of these, Stat3 predicted two potential target agents, OPB-111077 and ENMD-1198. OPB-111077 may enhance the body's immune attack against cancer cells by altering the signaling between cancer cells and surrounding cells, thus showing good effects in anti-cancer⁴¹. However, in clinical use, it may be limited by drug side effects as well as individual patient differences. Although ENMD-1198 has not been studied in the treatment of disease, because of its association with Stat3, it is speculated that it may have a similar anti-cancer mechanism to OPB-111077. 13 drugs predicted to target Homx1 may work by inhibiting or activating specific enzymes that affect cell growth and differentiation, which in turn affects signaling pathways within cells. For example, compounds such as D-alpha-Tocopherol acetate and Vitamin E may protect cells from free radical damage through antioxidant action, thus protecting cell membranes from oxidative damage⁴². The 34 drugs predicted by Egfr and 106 drugs predicted by Ptg2 may have a mechanism of action similar to some of the compounds in the Homx1 predicted drugs mentioned above, also by affecting intracellular signaling pathways^{43,44}. However, the specific pharmacological mechanisms of these drugs still need to be confirmed by further studies.

Regrettably, in our qRT-PCR results, the changes in Stat3 expression levels in brain tissue and blood after CIRI were inconsistent, however, increased expression in blood was consistent with the changes in both the training and validation sets. We will explore in depth the mechanisms underlying the discrepancy between blood and tissue in future studies. However, a study demonstrated that the expression level of p-STAT3 protein increased in rats with CIRI compared with the sham-operated group²⁵. We speculate that STAT3 activation is mainly through increased phosphorylation rather than a direct increase in expression after CIRI. More and more studies indicate that p-STAT3 can promote angiogenesis, mediate cell survival, antagonize inflammation and apoptosis in the stroke⁴⁵. Specific cytokines bind to EGFR, resulting in receptor dimerization, the recruitment of JAKs and consequent phosphorylation and activation of JAKs which leads to activation of the STAT proteins via phosphorylation⁴⁵. Our results showed strong interaction between Stat3 and the other three biomarkers in CIRI model, as well as differentially expressed molecules in the upstream and downstream of the STAT3 pathways, which would provide data basis for clarifying the effect of Stat3 in the process of CIRI.

The changes in Ptg2 expression levels between the training and validation sets were inconsistent, however, increased Ptg2 expression in our qRT-PCR results was consistent with the changes in training sets. Ptg2 encodes the PTGS2, which is the rate-limiting enzyme in the biosyntheses of prostaglandin G/H synthase⁴⁶. A study indicated that brief preconditioning of myocardial ischemia/reperfusion induced activation of PTGS2 and STAT3, which together contributed to protection against ischemia-reperfusion injury⁴⁷. Another study reported that Ptg2 served as ferroptosis-related biomarkers for ischemic stroke⁴⁸.

At present, there are still some shortcomings in the study of antiangiogenic drug therapy. First, the therapy is short-lived because of the redundancy of targets or mechanisms against neovascularization and the presence of intrinsic resistance or resistance to specific drugs. Secondly, there are large differences within tissues, and the inconsistency of sample sampling, processing and preservation will interfere with the accuracy of biomarker detection. In addition, there is a lack of uniformity in biomarker measurement techniques across studies and clinical settings, leading to bias in results. Finally, the accuracy of existing prognostic models in predicting individual clinical outcomes is insufficient. Due to the high heterogeneity of individuals, it is difficult for models to comprehensively consider multiple factors of individuals. These limitations may also be present in the treatment of CIRI with a regimen of stimulating angiogenesis. Despite these limitations, our study also provides a new perspective or data support for the mechanism and development of CIRI angiogenesis therapy and has a positive future outlook. Although there are limited reports on the resistance of pro-angiogenic drugs, the biomarkers screened in this study may also be promising for monitoring the treatment of tumor anti-angiogenesis drugs. For anti-angiogenic therapy, it is necessary to explore the resistance mechanism, based on the results of biomarker and resistance mechanism studies, further study the relationship between pathways, combined with immunotherapy or targeted therapy, in order to improve the therapeutic effect and reduce the generation of drug resistance. In addition, standardized sample collection, processing, and preservation processes need to be adopted to take heterogeneity into account for accurate sampling to ensure consistency of results in different environments. The improvement of prognostic model can focus on incorporating more individual factors, combining clinical experience data and individual conditions of patients to formulate treatment plans, so that the study results are more suitable for clinical practical application. Therefore, it is necessary to further explore the role of CIRI biomarkers in angiogenesis therapy.

Conclusions

In this study, we focused on five biomarkers closely related to CIRI and analyzed the lncRNA-miRNA-mRNA network as well as targeted therapeutic agents for these biomarkers, providing a research basis for further understanding the pathological mechanism and treatment of CIRI.

Materials and methods

Acquisition of data

The GSE97537 (microarray data) training set (12 rat ipsilateral brain samples (seven CIRI samples and five control samples)), GSE61616 (microarray data, 10 rat ipsilateral brain samples (five CIRI samples and five control samples)) and GSE78731 (Microarray data, 11 rat ipsilateral brain samples (six CIRI samples and five control samples)) validation set were acquired via gene expression omnibus (GEO) (<https://www.ncbi.nlm.nih.gov/gds>) database. 181 angiogenesis-related genes (ARGs) (species originated from homo sapiens) were extracted

via Genecards database (<https://www.genecards.org/>) and molecular signatures database (MSigDB) (<https://www.gsea-msigdb.org/gsea/msigdb/index.jsp>).

Differential expression analysis and functional enrichment analysis

In the training set, DEGs between CIRI and control samples were sifted out by limma package (version 3.50.1)⁴⁹ setting adj. $P < 0.05$ and $|\log_2\text{FC}| > 0.1$. After that, 169 rat homologous genes were gained by converting ARGs. Differentially expressed ARGs (DE-ARGs) were acquired by taking the intersection of DEGs with rat homologous genes ($n = 169$), then, gene ontology (GO) and kyoto encyclopedia of genes and genomes (KEGG) enrichment analyses were performed on them by ClusterProfiler package (version 4.0.5)^{50–53}.

Screening and evaluation of biomarkers

First, random forest (RF) and extreme gradient boosting (XGBoost) analyses were performed on DE-ARGs to acquire corresponding genes respectively. Based on the obtained DE-ARGs, they were analysed using random forest (RF) and extreme gradient boosting (XGBoost) algorithms to obtain the corresponding genes. Random Forest is a supervised learning algorithm that is an integrated learning algorithm with decision tree based learner. It can be used for classification problems, regression problems, and solving model overfitting problems. Random Forest's ability to handle high-dimensional data and feature importance assessment capabilities make it well suited for this study. It is capable of filtering out features that are more important for distinguishing cell types and identifying biomarkers from a large number of potential features, thus indirectly reducing the effective dimensionality of the data and improving our understanding of the data and the accuracy of the model. By using the R package 'randomForest' (version 4.7-1)⁵⁴, the random forest analysis of DE-ARGs is performed to obtain the importance ranking of genes, and the genes whose importance is not 0 are selected as the genes obtained from the random forest screening. The XGBoost algorithm, which is a gradient boosting strategy with a very good generalisation ability, is an important algorithm in the field of machine learning. That is, it uses multiple trees to make decisions together, and the result of each tree is the difference between the target value and the prediction results of all previous trees, and add up all the results to get the final result, so as to achieve the enhancement of the effect of the whole model, screen out the features that are important for the research objectives, and reduce the complexity of the data. By using the R package "XGBoost" (version 1.6.2.1)⁵⁵, the DE-ARGs genes were analysed by XGBoost to obtain the importance ranking of the genes, and according to the results, the genes whose importance was not 0 were selected as the genes screened by XGBoost. Next, the genes obtained by these two machine learning methods were intersected to derive biomarkers. Finally, the expression levels of biomarkers were analyzed between CIRI and control samples in training set, and the results were validated by validation set. Moreover, in order to evaluate the diagnostic ability of biomarkers for CIRI, the receiver operating characteristic (ROC) curves were plotted by pROC package (version 1.18.0)⁵⁶ in the training and validation set.

Functional enrichment analysis, tissue-specific expression and protein protein interaction (PPI) network of biomarkers

In order to explore the biological functions and signaling pathways involved in the biomarkers, we performed ingenuity pathway analysis (IPA) on them. The training set samples were divided into high/low expression groups according to the median value of biomarker expression levels, and gene set enrichment analysis (GSEA) was implemented on these two groups. Furthermore, the BioGPS (<http://biogps.org>) website was utilized to analyze the tissue-specific expression of biomarkers, and PPI network was constructed through GeneMANIA website (<https://www.biostars.org/p/271138/>).

Immune microenvironment analysis

The abundance of 28 immune cells in the training set was analyzed by ssGSEA, and we compared the differences in immune cell expression between CIRI and control samples. Next, Spearman correlation analysis was performed for biomarkers and immune cells with markedly different expression ($|\text{Cor}| > 0.3$ and $P < 0.05$).

Construction of competing endogenous RNA (ceRNA) and drug-target networks

To begin with, the mirwalk database (<http://mirwalk.umm.uni-heidelberg.de/>) was utilized to predict miRNAs targeted by the biomarkers. Afterwards, the genes targeted by the miRNAs were predicted by multiMiR package (version 1.16.0)⁵⁷, and the lncRNAs were extracted according to the gtf annotation file of rats (*Rattus norvegicus*. Rnor_6.0.96.gtf). Then, we construct a ceRNA network through Cytoscape software. Finally, potential therapeutic drugs for biomarkers were gained via DrugBank database (<https://go.drugbank.com/drugs>), and we constructed a drug-target network.

Quantitative real-time polymerase chain reaction (qRT-PCR) of blood and tissue samples

The SPF healthy male SD rats were obtained from Beijing Vital River Laboratory Animal Technology Co., Ltd. They were adaptively fed for a week in a comfortable environment with SPF and access to food and water. Rats weighed 250–280 g when used. Rats were anaesthetized with isoflurane (Ruiwode, Shenzhen, China), and the induction and maintenance concentrations were 3.5% and 1.5% respectively. In the model group, a silicone-coated nylon monofilament (Ruiwode) was inserted into the internal carotid artery via the right common carotid artery until the ipsilateral middle cerebral artery (MCA) was occluded, which induced focal cerebral ischemia. Blood reperfusion was performed by withdrawing the filament 90 min later, then the right common carotid artery was ligated. The experimental procedures for treating rats in the control group were identical except that the MCAs were not occluded. Longa scale was used to evaluate the successful establishment of animal models. The brains of the rats were removed quickly after blood collection from their hearts. The 11 fresh rat whole blood samples were divided into CIRI group ($N = 7$) and Control group ($N = 4$). The 11 frozen brain tissue

samples of rat were divided into CIRI group ($N=6$) and Control group ($N=5$). Experimental procedures were performed in accordance with the National Institute of Health Guide for the Care and Use of Experimental Animals, and the animal protocol was approved by the Medical Ethics Review Committee of Xi'an Medical University (May 11th, 2023./No. XYLS2023084). All methods were performed in accordance with the relevant guidelines and regulations, as well as in accordance with the ARRIVE guidelines. Next, the total RNA of blood and tissue samples was extracted with TRIzol reagent. We separately took 1 μ l RNA of blood and tissue samples and detected the concentration of them with NanoPhotometer N50. The mRNAs of blood and tissue samples were reverse transcribed using the surescript-first-strand-cDNA-synthesis-kit from Servicebio company. The reverse transcription product cDNA was diluted 5–20 times with ddH₂O (RNase/DNase free), and then the qPCR reaction was subjected. The internal reference for gene detection was GAPDH. Finally, the expressions of biomarkers between CIRI and Control groups were compared. Primer sequences of blood and tissue samples were shown in Table S1.

Data availability

Data Availability: The original data presented in the study are openly available in [Genecards database and MSigDB] at [<https://www.ncbi.nlm.nih.gov/gds>, <https://www.gsea-msigdb.org/gsea/msigdb/index.jsp>].

Received: 28 August 2024; Accepted: 17 December 2024

Published online: 30 December 2024

References

- Huang, L. et al. Curcumin alleviates cerebral ischemia-reperfusion Injury by inhibiting NLRP1-dependent neuronal pyroptosis. *Curr. Neurovasc Res.* **18**, 189–196. <https://doi.org/10.2174/1567202618666210607150140> (2021).
- Lim, S. et al. Senolytic therapy for cerebral ischemia-reperfusion Injury. *Int. J. Mol. Sci.* **22** <https://doi.org/10.3390/ijms222111967> (2021).
- Chen, S. J., Yuan, X. Q., Xue, Q., Lu, H. F. & Chen, G. Current research progress of isoflurane in cerebral ischemia/reperfusion injury: a narrative review. *Med. Gas Res.* **12**, 73–76. <https://doi.org/10.4103/2045-9912.330689> (2022).
- Montaner, J. et al. Multilevel omics for the discovery of biomarkers and therapeutic targets for stroke. *Nat. Rev. Neurol.* **16**, 247–264. <https://doi.org/10.1038/s41582-020-0350-6> (2020).
- Stamova, B. et al. Gene expression profiling of blood for the prediction of ischemic stroke. *Stroke* **41**, 2171–2177. <https://doi.org/10.1161/STROKEAHA.110.588335> (2010).
- Zhan, X. et al. Transient ischemic attacks characterized by RNA profiles in blood. *Neurology* **77**, 1718–1724. <https://doi.org/10.1212/WNL.0b013e318236ee66> (2011).
- Jickling, G. C. et al. Ischemic transient neurological events identified by immune response to cerebral ischemia. *Stroke* **43**, 1006–1012. <https://doi.org/10.1161/STROKEAHA.111.638577> (2012).
- Khamchai, S. et al. Morin Attenuated Cerebral Ischemia/Reperfusion Injury through promoting angiogenesis mediated by Angiopoietin-1-Tie-2 Axis and Wnt/beta-Catenin pathway. *Neurotox. Res.* **40**, 14–25. <https://doi.org/10.1007/s12640-021-00470-7> (2022).
- Krupinski, J., Kaluza, J., Kumar, P., Kumar, S. & Wang, J. M. Role of angiogenesis in patients with cerebral ischemic stroke. *Stroke* **25**, 1794–1798. <https://doi.org/10.1161/01.str.25.9.1794> (1994).
- Hayashi, T., Noshita, N., Sugawara, T. & Chan, P. H. Temporal profile of angiogenesis and expression of related genes in the brain after ischemia. *J. Cereb. Blood Flow. Metab.* **23**, 166–180. <https://doi.org/10.1097/01.WCB.0000041283.53351.CB> (2003).
- Su, X. et al. Governor vessel-unblocking and mind-regulating' acupuncture therapy ameliorates cognitive dysfunction in a rat model of middle cerebral artery occlusion. *Int. J. Mol. Med.* **43**, 221–232. <https://doi.org/10.3892/ijmm.2018.3981> (2019).
- Wu, Y. et al. Electric Acupuncture Treatment Promotes Angiogenesis in rats with Middle cerebral artery occlusion through EphB4/EphrinB2 mediated Src/PI3K Signal Pathway. *J. Stroke Cerebrovasc. Dis.* **30**, 105165. <https://doi.org/10.1016/j.jstrokecerebrovasdis.2020.105165> (2021).
- Hasan, T. F. et al. Diagnosis and management of Acute ischemic stroke. *Mayo Clin. Proc.* **93**, 523–538. <https://doi.org/10.1016/j.mayocp.2018.02.013> (2018).
- Poittevin, M. et al. Diabetic microangiopathy: impact of impaired cerebral vasoreactivity and delayed angiogenesis after permanent middle cerebral artery occlusion on stroke damage and cerebral repair in mice. *Diabetes* **64**, 999–1010. <https://doi.org/10.2337/db14-0759> (2015).
- Peng, L. et al. Isoflurane post-conditioning ameliorates cerebral Ischemia/Reperfusion Injury by enhancing Angiogenesis through activating the Shh/Gli signaling pathway in rats. *Front. Neurosci.* **13**, 321. <https://doi.org/10.3389/fnins.2019.00321> (2019).
- Zhang, C. et al. Ultrasound-enhanced Protective Effect of Tetramethylpyrazine via the ROS/HIF-1A signaling pathway in an in Vitro Cerebral Ischemia/Reperfusion Injury Model. *Ultrasound Med. Biol.* **44**, 1786–1798. <https://doi.org/10.1016/j.ultrasmedbio.2018.04.005> (2018).
- Yang, Y. & Torbey, M. T. Angiogenesis and blood-brain barrier permeability in vascular remodeling after stroke. *Curr. Neuropharmacol.* **18**, 1250–1265. <https://doi.org/10.2174/1570159X18666200720173316> (2020).
- Lopes-Coelho, F., Martins, F., Pereira, S. A. & Serpa, J. Anti-angiogenic therapy: current challenges and Future perspectives. *Int. J. Mol. Sci.* **22** <https://doi.org/10.3390/ijms22073765> (2021).
- Tian, W., Cao, C., Shu, L. & Wu, F. Anti-angiogenic therapy in the treatment of Non-small Cell Lung Cancer. *Oncol Targets Ther.* **13**, 12113–12129. <https://doi.org/10.2147/ott.S276150> (2020).
- Wu, M. Y. et al. Current mechanistic concepts in Ischemia and Reperfusion Injury. *Cell. Physiol. Biochem.* **46**, 1650–1667. <https://doi.org/10.1159/000489241> (2018).
- Zlokovic, B. V. Neurovascular mechanisms of Alzheimer's neurodegeneration. *Trends Neurosci.* **28**, 202–208. <https://doi.org/10.1016/j.tins.2005.02.001> (2005).
- Fang, J., Wang, Z. & Miao, C. Y. Angiogenesis after ischemic stroke. *Acta Pharmacol. Sin.* **44**, 1305–1321. <https://doi.org/10.1038/s41401-023-01061-2> (2023).
- He, P. et al. Periodic mechanical stress activates PKCdelta-Dependent EGFR mitogenic signals in rat chondrocytes via PI3K-Akt and ERK1/2. *Cell. Physiol. Biochem.* **39**, 1281–1294. <https://doi.org/10.1159/000447833> (2016).
- Fan, Q. W. et al. EGFR phosphorylates tumor-derived EGFRvIII driving STAT3/5 and progression in glioblastoma. *Cancer Cell.* **24**, 438–449. <https://doi.org/10.1016/j.ccr.2013.09.004> (2013).
- Tang, Y. et al. JAK2/STAT3 pathway is involved in the protective effects of epidermal growth factor receptor activation against cerebral ischemia/reperfusion injury in rats. *Neurosci. Lett.* **662**, 219–226. <https://doi.org/10.1016/j.neulet.2017.10.037> (2018).
- Zhou, J. et al. Crosstalk between MAPK/ERK and PI3K/AKT Signal pathways during Brain Ischemia/Reperfusion. *ASN Neuro.* **7** <https://doi.org/10.1177/1759091415602463> (2015).

27. Qian, J. et al. Transcriptomic Study Reveals Recovery of Impaired Astrocytes Contribute to Neuroprotective Effects of Danhong Injection against Cerebral Ischemia/Reperfusion-Induced Injury. *Front. Pharmacol.* **9**, 250. <https://doi.org/10.3389/fphar.2018.00250> (2018).
28. Berczki, D. Jr., Balla, J. & Berczki, D. Heme Oxygenase-1: clinical relevance in ischemic stroke. *Curr. Pharm. Des.* **24**, 2229–2235. <https://doi.org/10.2174/1381612824666180717101104> (2018).
29. Le, X. et al. Dual EGFR-VEGF pathway inhibition: a promising strategy for patients with EGFR-Mutant NSCLC. *J. Thorac. Oncol.* **16**, 205–215. <https://doi.org/10.1016/j.jtho.2020.10.006> (2021).
30. Fu, C. et al. Rehmannioside A improves cognitive impairment and alleviates ferroptosis via activating PI3K/AKT/Nrf2 and SLC7A11/GPX4 signaling pathway after ischemia. *J. Ethnopharmacol.* **289**, 115021. <https://doi.org/10.1016/j.jep.2022.115021> (2022).
31. Liu, C., Li, Z. & Xi, H. Bioinformatics analysis and in vivo validation of ferroptosis-related genes in ischemic stroke. *Front. Pharmacol.* **13**, 940260. <https://doi.org/10.3389/fphar.2022.940260> (2022).
32. Pan, L. et al. Network pharmacology and experimental validation-based approach to understand the effect and mechanism of Taohong Siwu decoction against ischemic stroke. *J. Ethnopharmacol.* **294**, 115339. <https://doi.org/10.1016/j.jep.2022.115339> (2022).
33. de Sa, K. S. G. et al. Gasdermin-D activation promotes NLRP3 activation and host resistance to Leishmania infection. *Nat. Commun.* **14**, 1049. <https://doi.org/10.1038/s41467-023-36626-6> (2023).
34. Rydbirk, R. et al. Brain proteome profiling implicates the complement and coagulation cascade in multiple system atrophy brain pathology. *Cell. Mol. Life Sci.* **79**, 336. <https://doi.org/10.1007/s00018-022-04378-z> (2022).
35. Lin, W. et al. Role of Calcium Signaling Pathway-Related Gene Regulatory Networks in ischemic stroke based on multiple WGCNA and single-cell analysis. *Oxid. Med. Cell. Longev.* **2021** (8060477). <https://doi.org/10.1155/2021/8060477> (2021).
36. Heljasvaara, R., Aikio, M., Ruotsalainen, H. & Pihlajaniemi, T. Collagen XVIII in tissue homeostasis and dysregulation - lessons learned from model organisms and human patients. *Matrix Biol.* **57–58**, 55–75. <https://doi.org/10.1016/j.matbio.2016.10.002> (2017).
37. Rakkar, K., Othman, O. A., Sprigg, N., Bath, P. M. & Bayraktutan, U. Evaluation of endothelial progenitor cell characteristics as clinical biomarkers for Elderly patients with ischaemic stroke. *Stem Cell. Rev. Rep.* **19**, 1856–1869. <https://doi.org/10.1007/s12015-023-10544-y> (2023).
38. Qian, S. et al. Plasma endostatin levels at Acute Phase of Ischemic Stroke are Associated with Post-stroke Cognitive Impairment. *Neurotox. Res.* **37**, 956–964. <https://doi.org/10.1007/s12640-020-00173-5> (2020).
39. Zhang, C. et al. Endostatin as a novel prognostic biomarker in acute ischemic stroke. *Atherosclerosis* **293**, 42–48. <https://doi.org/10.1016/j.atherosclerosis.2019.11.032> (2020).
40. Wu, J. et al. Synergic effect of PD-1 blockade and endostar on the PI3K/AKT/mTOR-mediated autophagy and angiogenesis in Lewis lung carcinoma mouse model. *Biomed. Pharmacother.* **125**, 109746. <https://doi.org/10.1016/j.biopha.2019.109746> (2020).
41. Yuan, S., Xu, Y., Yi, T. & Wang, H. The anti-tumor effect of OP-B on ovarian cancer in vitro and in vivo, and its mechanism: an investigation using network pharmacology-based analysis. *J. Ethnopharmacol.* **283**, 114706. <https://doi.org/10.1016/j.jep.2021.114706> (2022).
42. Galli, F. et al. Vitamin E (Alpha-Tocopherol) metabolism and Nutrition in chronic kidney disease. *Antioxid. (Basel)*. **11**. <https://doi.org/10.3390/antiox11050989> (2022).
43. Lee, M. J. et al. Vitamin D deficiency as a risk factor for sudden cardiac arrest: a multicenter case-control study. *Nutr. Metab. Cardiovasc. Dis.* **34**, 2182–2189. <https://doi.org/10.1016/j.numecd.2024.05.007> (2024).
44. Zhang, J. et al. Menaquinone-4 attenuates ferroptosis by upregulating DHODH through activation of SIRT1 after subarachnoid hemorrhage. *Free Radic Biol. Med.* **210**, 416–429. <https://doi.org/10.1016/j.freeradbiomed.2023.11.031> (2024).
45. Liang, Z. et al. The emerging role of signal transducer and activator of transcription 3 in cerebral ischemic and hemorrhagic stroke. *Prog Neurobiol.* **137**, 1–16. <https://doi.org/10.1016/j.pneurobio.2015.11.001> (2016).
46. Jiang, J. & Yu, Y. Small molecules targeting cyclooxygenase/prostanoid cascade in experimental brain ischemia: do they translate? *Med. Res. Rev.* **41**, 828–857. <https://doi.org/10.1002/med.21744> (2021).
47. Bolli, R., Dawn, B. & Xuan, Y. T. Role of the JAK-STAT pathway in protection against myocardial ischemia/reperfusion injury. *Trends Cardiovasc. Med.* **13**, 72–79. [https://doi.org/10.1016/s1050-1738\(02\)00230-x](https://doi.org/10.1016/s1050-1738(02)00230-x) (2003).
48. Chen, G., Li, L. & Tao, H. Bioinformatics Identification of ferroptosis-related biomarkers and therapeutic compounds in ischemic stroke. *Front. Neurol.* **12**, 745240. <https://doi.org/10.3389/fneur.2021.745240> (2021).
49. Wang, Y., Wang, Z., Sun, J. & Qian, Y. Identification of HCC Subtypes with different prognosis and metabolic patterns based on Mitophagy. *Front. Cell. Dev. Biol.* **9**, 799507. <https://doi.org/10.3389/fcell.2021.799507> (2021).
50. Yu, G., Wang, L. G., Han, Y. & He, Q. Y. clusterProfiler: an R package for comparing biological themes among gene clusters. *OMICS* **16**, 284–287. <https://doi.org/10.1089/omi.2011.0118> (2012).
51. Kanehisa, M. & Goto, S. KEGG: kyoto encyclopedia of genes and genomes. *Nucleic Acids Res.* **28**, 27–30. <https://doi.org/10.1093/nar/28.1.27> (2000).
52. Kanehisa, M. Toward understanding the origin and evolution of cellular organisms. *Protein Sci.* **28**, 1947–1951. <https://doi.org/10.1002/pro.3715> (2019).
53. Kanehisa, M., Furumichi, M., Sato, Y., Kawashima, M. & Ishiguro-Watanabe, M. KEGG for taxonomy-based analysis of pathways and genomes. *Nucleic Acids Res.* **51**, D587–d592. <https://doi.org/10.1093/nar/gkac963> (2023).
54. Chen, C. et al. XGBoost-based machine learning test improves the accuracy of hemorrhage prediction among geriatric patients with long-term administration of rivaroxaban. *BMC Geriatr.* **23**, 418. <https://doi.org/10.1186/s12877-023-04049-z> (2023).
55. Ahmed, H., Soliman, H. & Elmogy, M. Early detection of Alzheimer's disease using single nucleotide polymorphisms analysis based on gradient boosting tree. *Comput. Biol. Med.* **146**, 105622. <https://doi.org/10.1016/j.combiomed.2022.105622> (2022).
56. Robin, X. et al. pROC: an open-source package for R and S+ to analyze and compare ROC curves. *BMC Bioinform.* **12**, 77. <https://doi.org/10.1186/1471-2105-12-77> (2011).
57. Ru, Y. et al. The multiMiR R package and database: integration of microRNA-target interactions along with their disease and drug associations. *Nucleic Acids Res.* **42**, e133. <https://doi.org/10.1093/nar/gku631> (2014).

Acknowledgements

This study was grateful for supported by Natural Science Foundation of Shanxi Province 2024JC-YBMS-695 and Key Disciplines of Xi'an Medical University 12202306 (Medical technology).

Author contributions

X.-Y.L. reviewed conceptualization, format. Y.-H.W., J.S. and J.H.H. prepared Figs. 1, 2, 3, 4, 5, 6 and 7. J.S. and Y.-H.W.; J.-H.H.I applied software and bioinformatics methods for data analysis. Y.-H.W. wrote the main manuscript text. All authors have seen and approved the final version of the manuscript being submitted.

Funding

This research was funded by Natural Science Foundation of Shanxi Province 2024JC-YBMS-695 and Key Disciplines of Xi'an Medical University 12202306 (Medical technology).

Declarations

Competing interests

The authors declare no competing interests.

Additional information

Supplementary Information The online version contains supplementary material available at <https://doi.org/10.1038/s41598-024-83783-9>.

Correspondence and requests for materials should be addressed to X.-Y.L.

Reprints and permissions information is available at www.nature.com/reprints.

Publisher's note Springer Nature remains neutral with regard to jurisdictional claims in published maps and institutional affiliations.

Open Access This article is licensed under a Creative Commons Attribution-NonCommercial-NoDerivatives 4.0 International License, which permits any non-commercial use, sharing, distribution and reproduction in any medium or format, as long as you give appropriate credit to the original author(s) and the source, provide a link to the Creative Commons licence, and indicate if you modified the licensed material. You do not have permission under this licence to share adapted material derived from this article or parts of it. The images or other third party material in this article are included in the article's Creative Commons licence, unless indicated otherwise in a credit line to the material. If material is not included in the article's Creative Commons licence and your intended use is not permitted by statutory regulation or exceeds the permitted use, you will need to obtain permission directly from the copyright holder. To view a copy of this licence, visit <http://creativecommons.org/licenses/by-nc-nd/4.0/>.

© The Author(s) 2024